1-2009

Mutation of H63 and its Catalytic Affect on the Methionine Aminopeptidase from *Escherichia coli*

Sanghamitra Mitra
Loyola University Chicago

Brian Bennett
Medical College of Wisconsin

Richard C. Holz
Marquette University

Mutation of H63 and Its Catalytic Affect On the Methionine Aminopeptidase from *Escherichia coli*

Sanghamitra Mitra
Department of Chemistry, Boston University, Boston, MA
Brian Bennett
Department of Biophysics, Medical College of Wisconsin, Milwaukee, WI
Richard C. Holz
Department of Chemistry, Loyola University Chicago, Chicago, IL

Abstract: In order to gain insight into the mechanistic role of a flexible exterior loop near the active site, made up of Y62, H63, G64, and Y65, that has been proposed to play an important role in substrate binding and recognition in the methionyl aminopeptidase from *Escherichia coli* (*Ec*MetAP-I), the H63A enzyme was prepared. Mutation of H63 to alanine does not affect the ability of the enzyme to bind divalent metal ions. The specific activity of H63A *Ec*MetAP-I was determined using four different substrates of varying lengths, namely, L-Met-*p*-NA, MAS, MGMM and MSSHRWDW. For the smallest/shortest substrate (L-Met-*p*-NA) the specific activity decreased nearly seven fold but as the peptide length increased, the specific activity also increased and became comparable to WT *Ec*MetAP-I. This decrease in specific activity is primarily due to a decrease in the observed k_{cat} values, which decreases nearly sixty-fold for L-Met-*p*-NA while only a four-fold decrease is

Biochimica et Biophysica Acta: Proteins and Proteomics, Vol. 1794, No. 1 (January 2009): pg. 137-143. DOI.

observed for the tri- and tetra-peptide substrates. Interestingly, no change in k_{cat} was observed when the octa-peptide MSSHRWDW was used as a substrate. These data suggest that H63 affects the hydrolysis of small peptide substrates whereas large peptides can overcome the observed loss in binding energy, as predicted from K_m values, by additional hydrophilic and hydrophobic interactions.

Keywords: Enzymology, Enzyme kinetic, Methionine aminopeptidase, Cobalt

Methionine aminopeptidases (MetAPs) represent a unique class of protease that are responsible for removing the N-terminal methionine residue from proteins and polypeptide chains [1-5]. Methionine free N-termini have been postulated to be important for additional protein processing to occur, such as removal of signal sequences (if present), proteolytic cleavage to generate shorter peptides, or the covalent attachment of residues and blocking groups such as acetyl and myristoyl groups [1]. MetAPs are therefore one of the key cellular enzymes involved in protein maturation [5,6]. The physiological importance of MetAP is underscored by the lethality of the absence of all the genes or the gene products in *Escherichia coli* (*Ec*MetAP-I). *Salmonella typhimurium* and *Saccharomyces cerevisiae* [7-10]. Moreover, based on fumagillin affinity chromatography and mass spectrometry, MetAPs were identified as the molecular targets of fumagillin and TNP-470 [11,12]. *In vivo* studies showed that one of the observed effects of inhibiting MetAPs by anti-angiogenesis agents is the failure to expose glycine residues at the N-termini of certain signaling proteins involved in cell cycle regulation, which prevents myristolyation [13]. Therefore, MetAPs represent an extremely promising target for the design of a novel class of anti-angiogenesis drugs, some of which are currently under clinical investigation [11,14-19].

MetAPs are organized into two classes (types-I and -II) based on the absence or presence of an extra 62 amino acid sequence (of unknown function) inserted near the catalytic domain. The type-I MetAPs from *E. coli* (Ec*MetAP-I*), *Staphylococcus aureus* (Sa*MetAP-I*), *Homo sapiens* (Hs*MetAP-I)*, and *Thermotoga maritima* (Tm*MetAP-I*) and the type-II MetAPs from *H. sapiens* (Hs*MetAP-II*) and *Pyrococcus furiosus* (Pf*MetAP-II*) have been crystallographically characterized [17,20-26]. All six display a novel "pita-bread" fold with an internal pseudo two-fold symmetry that structurally relates the first and

second halves of the polypeptide chain to each other. Each half contains an antiparallel β-pleated sheet flanked by two helical segments and a C-terminal loop. Both domains contribute conserved residues to the metallo-active site. In all six structures, a bis(μ-carboxylato)(μ-aquo/hydroxo) dicobalt core is observed with an additional carboxylate residue at each metal site and a single histidine bound to Co1. Recently, an X-ray crystal structure of EcMetAP-I was reported with partial occupancy (40%) of a single Mn(II) ion bound in the active site [27]. This structure was obtained by adding the transition-state analog inhibitor l-norleucine phosphonate (l -NleP), in order to impede divalent metal binding to the second site, and by limiting the amount of metal ion present during crystal growth. This structure provides the first structural verification that MetAPs can form mononuclear active sites and the single divalent metal ion resides the H171 side of the active site as previously predicted by ^{1}H NMR and EXAFS spectroscopy [28,29].

All MetAPs appear to have similar substrate specificites that are dictated by the penultimate residue. MetAPs will only remove N-terminal methionine residues from polypetide chains (P1) and only if the amino acid residue adjacent to the N-terminal methionine (P1′) is physically small and/or uncharged (*e.g.* G, A, P, S, T, C and V) [30]. MetAP substrate preference is opposite to the "N-end rule" for protein degradation since MetAPs will not remove an N-terminal methionine if a "destabilizing" amino acid will be exposed [31,32]. In cases where the N-terminal methionine residue is retained, it has been postulated to act as a prophylactic cap preventing premature degradation [31,32]. At this time it is unclear whether MetAPs have P2′ or P3′ recognition sites, but in previous studies with the substrate MSSHRWDW that has six residues downstream from the P1′ site, the Michaelis-Menten constant (K_m) was found to be ~10 and ~3 orders of magnitude lower compared to three- and four-residue substrates, respectively [33]. A flexible loop near the active site of all bacterial MetAPs, made up of Y62, H63, G64, and Y65 (*E. coli* numbering) has been proposed to play an important role in substrate binding and recognition and may provide a route to selective inhibition of bacterial *vs.* mammalian MetAP enzymes [22,25]. In *Ec*MetAP-I, H63 appears to form a "cap" over the substrate binding channel (Figs. 1A, B) [22]. The histidine at position-63 is strictly conserved in gram-negative bacteria including enterobacteria while in gram-positive bacteria the histidine is

Biochimica et Biophysica Acta: Proteins and Proteomics, Vol. 1794, No. 1 (January 2009): pg. 137-143. DOI.

replaced by tyrosine with the exception of SaMetAP-I, which has a glutamate at this position (Fig. 2). In order to investigate the role of this flexible loop in substrate recognition and catalysis we have prepared and characterized the H63A EcMetAP-I enzyme.

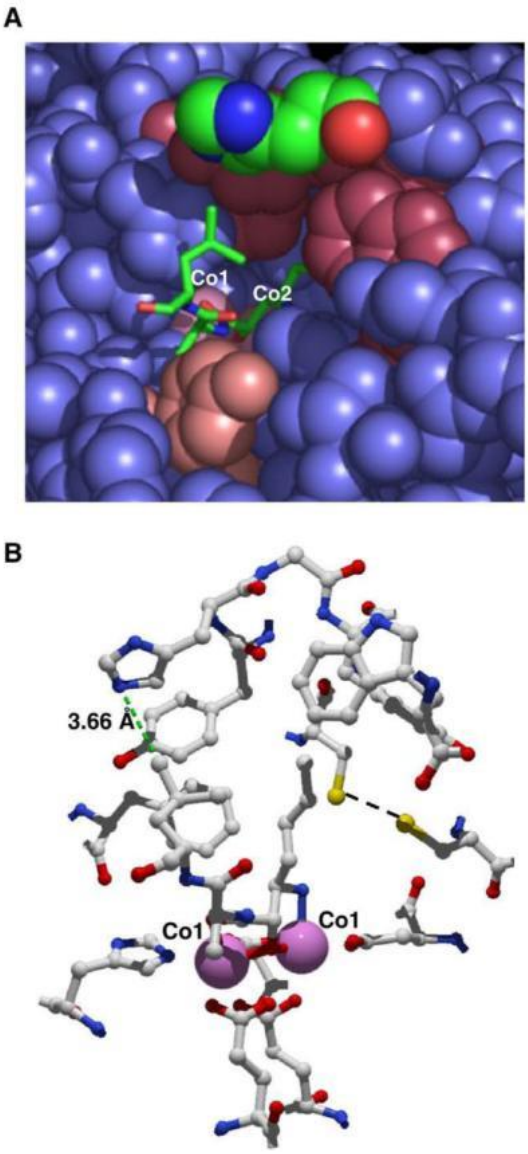

Fig. 1
(A)Space-filling model of *Ec*MetAP-I complexed with the substrate-analog inhibitor (3R)-amino-(2S)-hydroxyheptanoyl- l-Ala- l-Leu- l-Val- l-Phe-OMe (PDB: 3MAT). Color coding: H63A (green, blue and red), S1 pocket residues (magenta), S2 pocket residues (dirty pink) and metal ions (pink). (B) *Ec*MetAP-I active site complexed with the substrate-analog inhibitor (3R)-amino-(2S)-hydroxyheptanoyl- l-Ala- l-Leu- l-Val- l-Phe-OMe (PDB: 3MAT). The H63 residue is 3.66 Å from the third residue of the substrate-analog inhibitor. (For interpretation of the references to colour in this figure legend, the reader is referred to the web version of this article.)

Biochimica et Biophysica Acta: Proteins and Proteomics, Vol. 1794, No. 1 (January 2009): pg. 137-143. DOI.

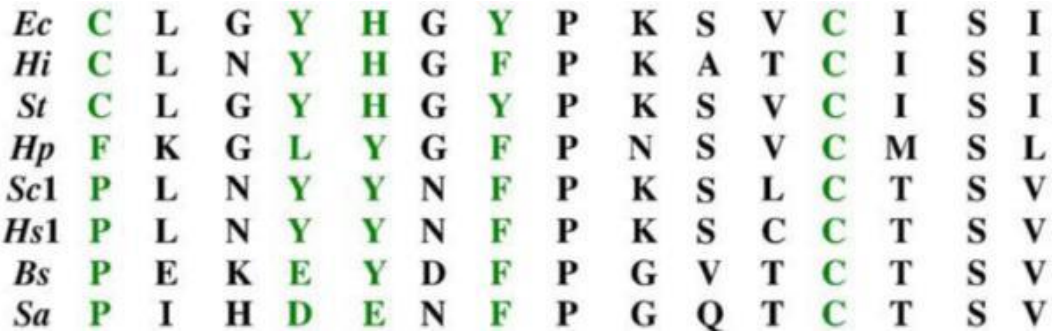

Fig. 2
Sequence alignment of select MetAP-Is. S1 pocket residues (green) (*Ec*) *Escherichia, coli*-I; (*St*) *Salmonella typhimurium*-I (all are enterobacteria) (*HI*) *Haemophilus, influenzae*-I; (*Hp*) *Helicobacter pylori*-I; (*Sc*) *Sacchromyce cerevisiae*-I; (*Hs*) *Homo sapiens*-I; (*Bs*) *Bacillus subtilis; (Sa) Staphylococcus aureus.* (For interpretation of the references to colour in this figure legend, the reader is referred to the web version of this article.)

1. Materials and methods

1.1. Mutagenesis, protein expression and purification

The H63A mutated form of *Ec*MetAP-I was obtained by PCR mutagenesis using the following primers: 5′-C CTC GGC TAT XXX GGC TAT CC-3′ and 5′-G GAG CCG ATA YYY CCG ATA YYY CCG ATA GG-3′ with GCG for XXX and CGC for YYY, which encodes for the H63A mutant. The H63 site directed mutant was obtained using the Quick Changer™ Site-Directed Mutagenesis Kit (Stratagene, La Jolla, CA) following Stratagene's procedure. Reaction products were transformed into *E. coli* XL1-Blue competent cells (recAl endA1 gyrA96 thi-l hsdR17supE44 relA1 lac [F′ proAB $lacI^qZ\Delta M15$ Tn10 (Tet^r)]), grown on LB-agarose plates containing kanamycin at a concentration of 50 μg/ml. A single colony of the mutant was grown in 50 ml LB containing 50 μg/ml of kanamycin. Plasmids were isolated using Wizard Plus Minipreps DNA purification kit (Promega, Madison, WI) or Qiaprep® Spin Miniprep kit (Qiagene, Valencia, CA). The mutation was confirmed by DNA sequencing. Plasmids containing the mutated *Ec*MetAP-I gene were transformed into *E. coli* BL21 Star™(DE3) (*F ompT hsd*S_B (*r*$_B$*m*$_B$) gal dcm *rne131* (DE3)) (Invitrogen, Carlsbad, CA) and stock cultures prepared. The variant was purified identical to the wild-type *Ec*MetAP-I enzyme [16,28]. Purified H63A *Ec*MetAP-I exhibited a single band on SDS-PAGE at M_r of 29,630. Protein concentrations were estimated from the absorbance at 280 nm using an extinction coefficient of

Biochimica et Biophysica Acta: Proteins and Proteomics, Vol. 1794, No. 1 (January 2009): pg. 137-143. DOI.

16,445 M^{-1} cm^{-1} [34]. Apo-H63A *Ec*MetAP-I was washed free of methionine using Chelex-100 treated methionine-free buffer (25 mM HEPES, pH 7.5, 150 mM KCI) and concentrated by microfiltration using a Centricon-10 (Amicon, Beverly, MA) prior to all kinetic assays. Individual aliquots of apo-H63A *Ec*MetAP-I were routinely stored at -80 °C or in liquid nitrogen until needed.

1.2. Metal content measurements

H63A *Ec*MetAP-I enzyme samples used in metal analyses were typically 30 μM. Apo-H63A *Ec*MetAP-I was incubated anaerobically with Co(II) ($CoCl_2$: ≥99.999% Strem Chemicals, Newburyport, MA) for 30 min prior to exhaustive anaerobic exchange into Chelex-100 treated HEPES buffer as previously reported [28]. Metal analyses were performed using inductively coupled plasma-atomic emission spectrometry (ICP-AES).

1.3. Discontinuous enzymatic assay of H63A EcMetAP-I

Enzymatic assays of H63A *Ec*MetAP-I were performed under strict anaerobic conditions in an inert atmosphere glove box (Ar/5% H_2, ≤1 ppm O_2; Coy Laboratories) with a dry bath incubator to maintain the temperature. Catalytic activities were determined with an error of ±5% in 25 mM HEPES buffer, pH 7.5, containing 150 mM KCl. The amount of product formation was determined by high-performance liquid chromatography (HPLC, Shimadzu LC-10A class-VP5). A typical assay involved the addition of 8 μL of Co(II)-loaded H63A *Ec*MetAP-I to a 32 μL substrate-buffer mixture at 30 °C for 1 min. The reaction was quenched by the addition of 40 μL of 1% trifluoroacetic acid solution (TFA). Elution of the product was monitored at 215 nm following separation on a C8 HPLC column (Phenomenex, Luna; 5 μm, 4.6×25 cm), as previously described [28].

1.4. Spectrophotometric enzymatic assay of H63A EcMetAP-I

A typical reaction with l-Methionine-*p*-nitroaniline (L-Met-*p*-NA) as the substrate was carried out at 30 °C in a narrow path (~100 μL) quartz cuvette containing 25 mM HEPES buffer, pH 7.5, and 150 mM

Biochimica et Biophysica Acta: Proteins and Proteomics, Vol. 1794, No. 1 (January 2009): pg. 137-143. DOI.

KCl in a Shimadzu UV-3101PC spectrophotometer equipped with a constant-temperature cell holder and an Isotemp 2013D water bath (Fisher Scientific, Pittsburgh,PA). The rate for background hydrolysis of the substrate was measured by monitoring the formation of *p*-NA continuously at 405 nm (ε = 10,800 M^{-1} cm^{-1}) in a cell with a 1 cm light path for 10 min. The enzymatic reaction was initiated by the addition of Co(II)-loaded WT and H63A *Ec*MetAP-I and the progress curves were monitored at 405 nm [35].

1.5. Isothermal titration calorimetry

Isothermal titration calorimetry (ITC) measurements were carried out on a MicroCal OMEGA ultrasensitive titration calorimeter. The divalent metal ion ($CoCl_2$) titrant and apo-H63A *Ec*MetAP-I solutions were prepared in Chelex-100 treated 25 mM HEPES buffer, pH 7.5, and 150 KCl. Stock buffer solutions were thoroughly degassed before each titration. The enzyme solution (70 μM) was placed in the calorimeter cell and stirred at 200 rpm to ensure rapid mixing. Typically, 3 μL of titrant was delivered over 7.6 s with a 5 min interval between injections to allow for complete equilibration. Each titration was continued until 4.5-6 equivalents. of Co(II) had been added to ensure that no additional complexes were formed in excess titrant. A background titration, consisting of the identical titrant solution but only the buffer solution in the sample cell, was subtracted from each experimental titration to account for heat of dilution. The data were analyzed with a two or three-site binding model by the Windows-based Origin software package supplied by MicroCal [36]. The equilibrium binding constant, K_a, and the enthalpy change ΔH, were used to calculate ΔG and ΔS using the Gibbs free energy relationship (Eq. (1)):

$$\Delta G^{o} - RT\ln[K_a] = \Delta H^{o} - T\Delta S^{o} \quad (1)$$

where R=1.9872 cal mol^{-1} K^{-1}. The relationship between K_a and K_d is defined as:

$$K_d = 1/K_a \quad (2)$$

Biochimica et Biophysica Acta: Proteins and Proteomics, Vol. 1794, No. 1 (January 2009): pg. 137-143. DOI.

1.6. Spectroscopic measurements

Electronic absorption spectra were recorded on a Shimadzu UV-3101PC spectrophotometer. The apo-H63A *Ec*MetAP-I samples used in spectroscopic measurements were made rigorously anaerobic prior to incubation with Co(II) ($CoCl_2$: ≥99.999% Strem Chemicals, Newburyport, MA) for ~ 30 min at 20-25 °C. Co(II)-containing samples were handled throughout in an anaerobic glove box (Ar/5% H_2, ≥1 ppm O_2; Coy Laboratories) until forzen. Electronic absorption spectra were normalized for the protein concentration and the absorption due to uncomplexed Co(II) ($\varepsilon_{512\ nm}$ = 6.0 M^{-1} cm^{-1}) [28]. Low-temperature EPR spectroscopy was performed using a Bruker ESP-300E spectrometer equipped with an ER 4116 DM dual mode X-band cavity and an Oxford Instruments ESR-900 helium flow cryostat. Background spectra recorded on a buffer sample were aligned with and subtracted from experimental spectra as in earlier work [37,38]. EPR spectra were recorded at microwave frequencies of approximately 9.65 GHz: precise microwave frequencies were recorded for each individual spectrum to ensure precise *g*-alignment. All Spectra were recorded at a 100 kHz modulation frequency. Other EPR running parameters are specified in the figure legends for individual samples. EPR simulations were carried out using matrix diagonalization (XSophe, Bruker Biospin), assuming a spin Hamiltonian $H=\beta g\cdot H\cdot S\cdot + S\cdot D\cdot S + S\cdot A\cdot I$, with S = 3/2 and $D \gg \beta gHS$ ($=h\nu$), where all of the variables have their usual meanings [39]. H63A *Ec*MetAP-I enzyme concentrations for EPR were ~ 1 mM and samples were frozen after incubation of with the appropriate amount of metal ion for 60 min at 25 °C.

2. Results

2.1. Metal content of H63A EcMetAP-I

The number of tightly bound divalent metal ions was determined for H63A *Ec*MetAP-I by ICP-AES analysis. Apo-enzyme samples (30 μM), to which 2-30 equivalents of Co(II) were added under anaerobic conditions, were dialyzed extensively for 3 h at 4 °C with Chelex-100 treated, metal-free HEPES buffer (25 mM HEPES, 150 mM KCl, pH

Biochimica et Biophysica Acta: Proteins and Proteomics, Vol. 1794, No. 1 (January 2009): pg. 137-143. DOI.

7.5). ICP-AES analysis revealed 1.0±0.1 equivalent of cobalt associated with the H63A *Ec*MetAP-I enzyme.

2.2. Kinetic properties of H63A EcMetAP-I

Kinetic parameters were determined for the Co(II)-loaded H63A *Ec*MetAP-I enzyme using l -Met-*p*-NA, MAS, MGMM, and MSSHRWDW as substrates (Table 1). Activity assays were performed in triplicate for 8-15 concentrations of each substrate (l-Met-*p*-NA 0 to 5 mM; MAS, 0-60 mM; MGMM, 0-12 mM; MSSHRWDW, 0-12 mM). For l-Met-*p*-NA, product formation was monitored spectrophotometrically at 405 nm [35] while product was quantified by HPLC for MAS, MGMM, and MSSHRWDW. Both K_m and k_{cat} values were obtained by nonlinear fitting of these data to the Michaelis-Menten equation. The observed K_m values for WT *Ec*MetAP-I decreased in the order MAS>MGMM>MSSHRWDW> L-Met-*p*-NA (Table 1). For WT *Ec*MetAP-I, the observed k_{cat} values increased in the order l-Met-*p*-NA⋘MAS<MGMM<MSSHRWDW (Table 1). Because the observed k_{cat} value is significantly smaller for l-Met-*p*-NA *vs.* the other three substrates used, the catalytic efficiencies (k_{cat}/K_m) increase in the order l-Met-*p*-NA<MAS<MGMM<MSSHRWDW (Table 1). A similar trend was observed for k_{cat} values obtained for H63A *Ec*MetAP-I (l-Met-*p*-NA<MAS<MGMM<MSSHRWDW) except that the observed k_{cat} values for H63A *Ec*MetAP-I were ~60 times lower for L-Met-*p*-NA but only ~4-fold lower for MAS and MGMM (Table 1). However, the observed k_{cat} value for the hydrolysis of MSSHRWDW by H63A *Ec*-MetAP-I was identical, within error, to WT *Ec*MetAP-I (Table 1). The observed K_m values for H63A *Ec*MetAP-I decreased in the order MAS>MGMM>MSSHRWDW> l-Met-*p*-NA (Table 1). Interestingly, the observed K_m for MAS increased to 15 from 12 mM while that of l-Met-*p*-NA decreased slightly from 0.44 to 0.33 μM. The observed K_m values for MGMM and MSSHRWDW were identical, within error, to those obtained for WT *Ec*MetAP-I [28].

Biochimica et Biophysica Acta: Proteins and Proteomics, Vol. 1794, No. 1 (January 2009): pg. 137-143. DOI.

Table 1: Kinetic constants for Co(II)-loaded *Ec*MetAP-I for various substrates at 30 °C

Enzyme	Kinetic constants	l-Met-*p*-NA	MAS	MGMM	MSSHRWDW
WT *Ec*MetAP-I	k_m (mM)	0.44±0.03	12.0±0.1	3.0±0.1	1.0±0.1
	k_{cat} (s^{-1})	0.006±0.003	11.0±0.3	18.3±0.3	84±1.0
	k_{cat}/k_m (M^{-1} s^{-1})	13.7	920	6100	84,000
	SA (U/mg)	0.013±0.003	20.5±1.0	36.0±3.0	167±8.0
H63A *Ec*MetAP-I	k_m (mM)	0.33±0.02	15.0±0.1	3.1±0.3	1.0±0.1
	k_{cat} (s^{-1})	0.0001±0.00005	3.0±0.3	4.8±0.3	70±1.0
	k_{cat}/k_m (M^{-1} s^{-1})	3.0	200	1532	70,000
	SA (U/mg)	0.002±0.001	7.5±1.0	9.5±1.0	140±9.0

2.3. Metal binding properties of H63A EcMetAP-I

In order to determine the number of tight metal binding sites and the affinity of these sites, both activity titrations and isothermal titration calorimetry (ITC), were used. The extent of hydrolytic activity exhibited by the H63A *Ec*MetAP-I enzyme was examined as a function of Co(II) concentration with both MGMM and l-Met-*p*-NA as substrates (Fig. 3; inset). The apo-H63A *Ec*MetAP-I enzyme was incubated for 30 min under strict anaerobic conditions at pH 7.5 with Co(II) (0 to 200 equivalents) after which k_{cat} values were obtained. The k_{cat} value increased as a function of Co(II) ion concentration and exhibited a maximum after the addition of only one equivalent of Co(II). Further additions of Co(II) resulted in little change in the observed k_{cat} value until four equivalents of Co(II) has been added. At this point, the addition of Co(II) became inhibitory. These data were fit to Eq. (3) (Fig. 3) [40]:

$$r = pC_S/(K_d + C_S) \tag{3}$$

where p is the number of sites for which interaction with a ligand is governed by the intrinsic dissociation constant K_d, C_s is the free metal concentration (Co_{free} in this case), and r is the binding function that was calculated by conversion of the fractional saturation (f_a) as previously described [28]. The free metal concentration was calculated from:

Biochimica et Biophysica Acta: Proteins and Proteomics, Vol. 1794, No. 1 (January 2009): pg. 137-143. DOI.

$$C_S = C_{TS} - rC_A \quad (4)$$

where C_{TS} and C_A are the total molar concentrations of metal and enzyme, respectively. The best fit obtained with either MGMM or l-Met-*p*-NA provided a *p* value of 1 and a K_d value of 0.15 μM (Fig. 3).

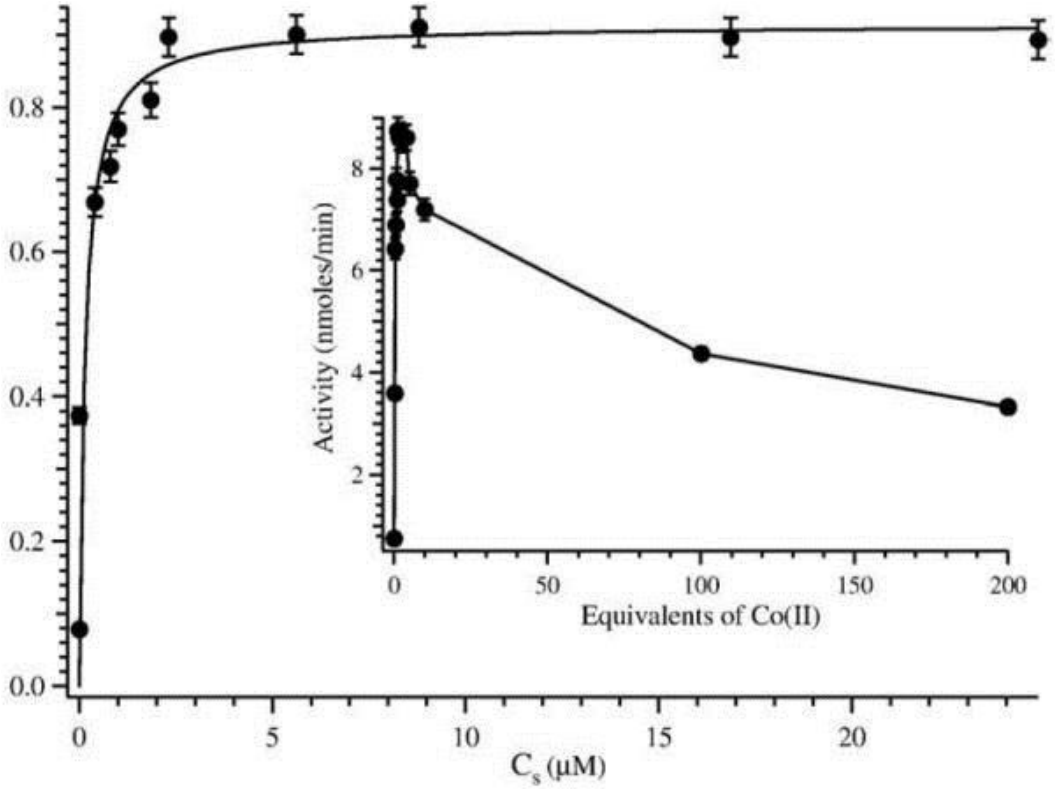

Fig. 3: Plot of binding function, *r vs.* C_s for the binding of Co(II) to H63A *Ec*MetAP-I using MGMM as the substrate in HEPES buffer at pH 7.5. The solid line is a fit to Eq. (3). Inset: plot of specific activity of *vs.* equivalents of added Co(II) ions.

Confirmation of the K_d value determined from enzymatic activity titrations for Co(II) binding to H63A *Ec*MetAP-I was obtained *via* ITC (Fig. 4). All ITC experiments were carried out at 25±0.2 °C and association constants (K_a) were obtained by fitting these data, after subtraction of the background heat of dilution, *via* an iterative process using the Origin software package. This software package uses a nonlinear least-squares algorithm, which allows the concentrations of the titrant and the sample to be fit to the heat-flow-per-injection to an equilibrium binding equation for two non-interacting sites. The K_a value, enzyme-metal stoichiometry (*n*), and the change in enthalpy

Biochimica et Biophysica Acta: Proteins and Proteomics, Vol. 1794, No. 1 (January 2009): pg. 137-143. DOI.

(Δ*H*°) were allowed to vary during the fitting process (Table 2, Fig. 4). The best fit obtained for H63A *Ec*MetAP-I provided an overall *n* value of 3 for two noninteracting sites, identical to WT *Ec*MetAP-I. Attempts to fit these data with *n* values of 1 or 2 provided poor fits. For H63A *Ec*MetAP-I, a K_d value of 5.8±1.2 μM was observed as well as two K_d values of 7.0±2.4 mM (Table 2). The first Co(II) binding event for H63A *Ec*MetAP-I was weakly endothermic while the second and third Co(II) binding events were significantly more endothermic.

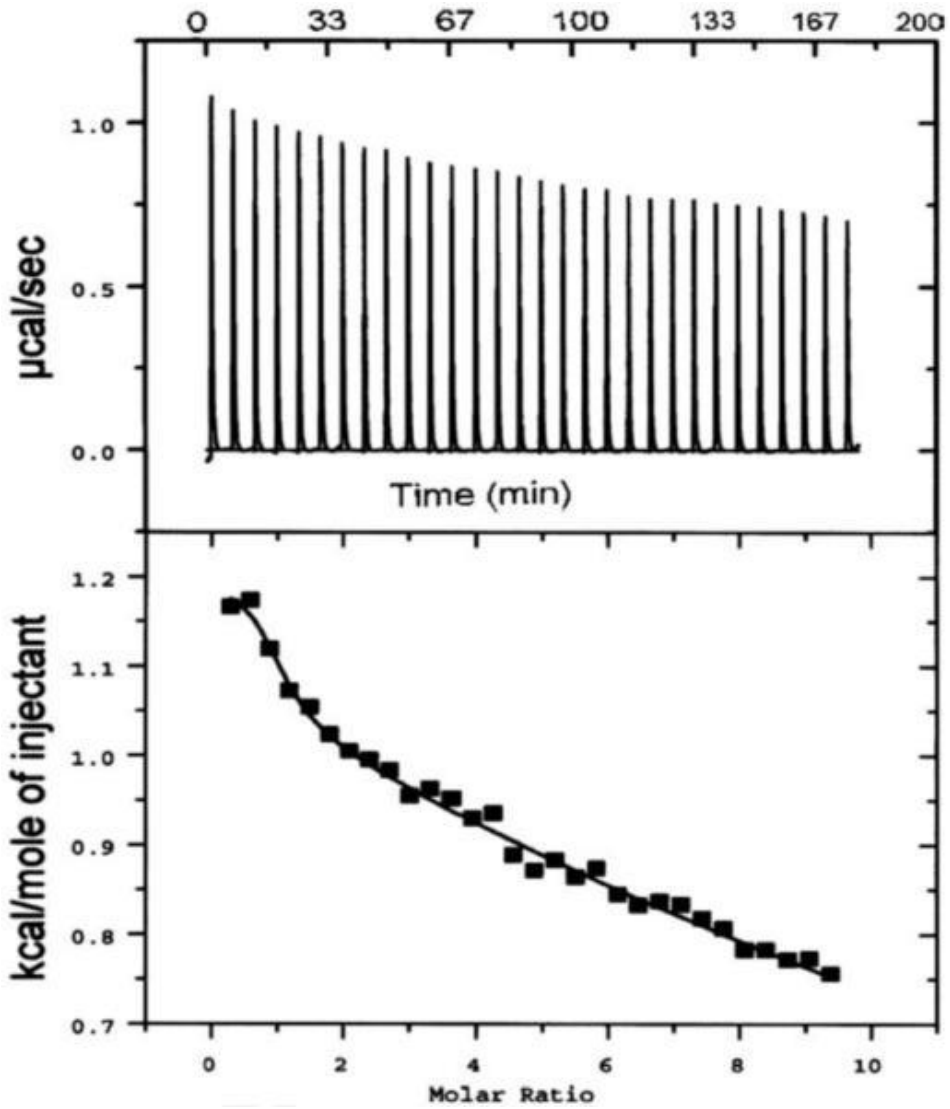

Fig. 4: (Top) ITC titration of a 70 μM solution of H63A *Ec*MetAP-I with a 5 mM Co(II) solution. (Bottom) Fit of the ITC data for H63A *Ec*MetAP-I. The fits were obtained using noninteracting sites model and provided an overall *n* value of 3, with one tight and two loose sites. Reaction conditions: 20 °C in 25 mM HEPES, pH 7.5, and 150 mM KCI.

Biochimica et Biophysica Acta: Proteins and Proteomics, Vol. 1794, No. 1 (January 2009): pg. 137-143. DOI.

Table 2: Dissociation constants (K_d), metal-enzyme stoichiometry (n) and thermodynamic parameters for Co(II) binding to both WT and H63A *Ec*MetAP-I

Enzyme	n	K_{d1}, K_{d2} (μM)	ΔH_1, ΔH_2 (kcal/mol)	$T\Delta S_1$, $T\Delta S_2$ (kcal/mol)	ΔG_1, ΔG_2 (kcal/mol)
WT *Ec*MetAP-I	1	6.4	15.4	20.3	-7.9
	2	14,000	1060	1060	-2.5
H63A *Ec*MetAP-I	1	5.8	1.19	8.29	-7.1
	2	7000	65.8	68.7	-2.9

For data with n=1, one Co(II) ion is tightly bound and n=2 represents two Co(II) ions binding to sites per protein.

2.4. Spectroscopic studies of Co(II)-loaded H63A EcMetAP-I

The electronic absorption spectra of H63A *Ec*MetAP-I, after the addition of one and two equivalents of Co(II), were recorded under strict anaerobic conditions in 25 mM HEPES buffer, pH 7.5 and 150 mM KCl (Fig. 5). The addition of one and two equivalents of Co(II) to apo-H63A *Ec*MetAP-I provided a complex spectra comprised of at least four bands between 500 and 700 nm with extinction coefficients ranging from 60 to 20 M^{-1} cm^{-1}. The EPR spectrum of a 1.5 mM H63A *Ec*MetAP-I sample in 25 mM HEPES, pH 7.5, and 150 mM KCl after the addition of 1 and 2 equivalents of Co(II) were indistinguishable from each other and from the corresponding spectra exhibited by WT Co(II)-loaded *Ec*MetAP-I (Figure S1) [28]. The spectrum of [CoCo(H63A-*Ec*MetAP-I)] accounted for 100%±5% of the added Co(II). The spectrum was broad (line widths>500 G) and exhibited no resolvable ^{59}Co hyperfine splitting, presumably due to the extensive strains in g and zero-field splitting parameters sometimes associated with high-spin S=3/2 Co(II) centers.

Biochimica et Biophysica Acta: Proteins and Proteomics, Vol. 1794, No. 1 (January 2009): pg. 137-143. DOI.

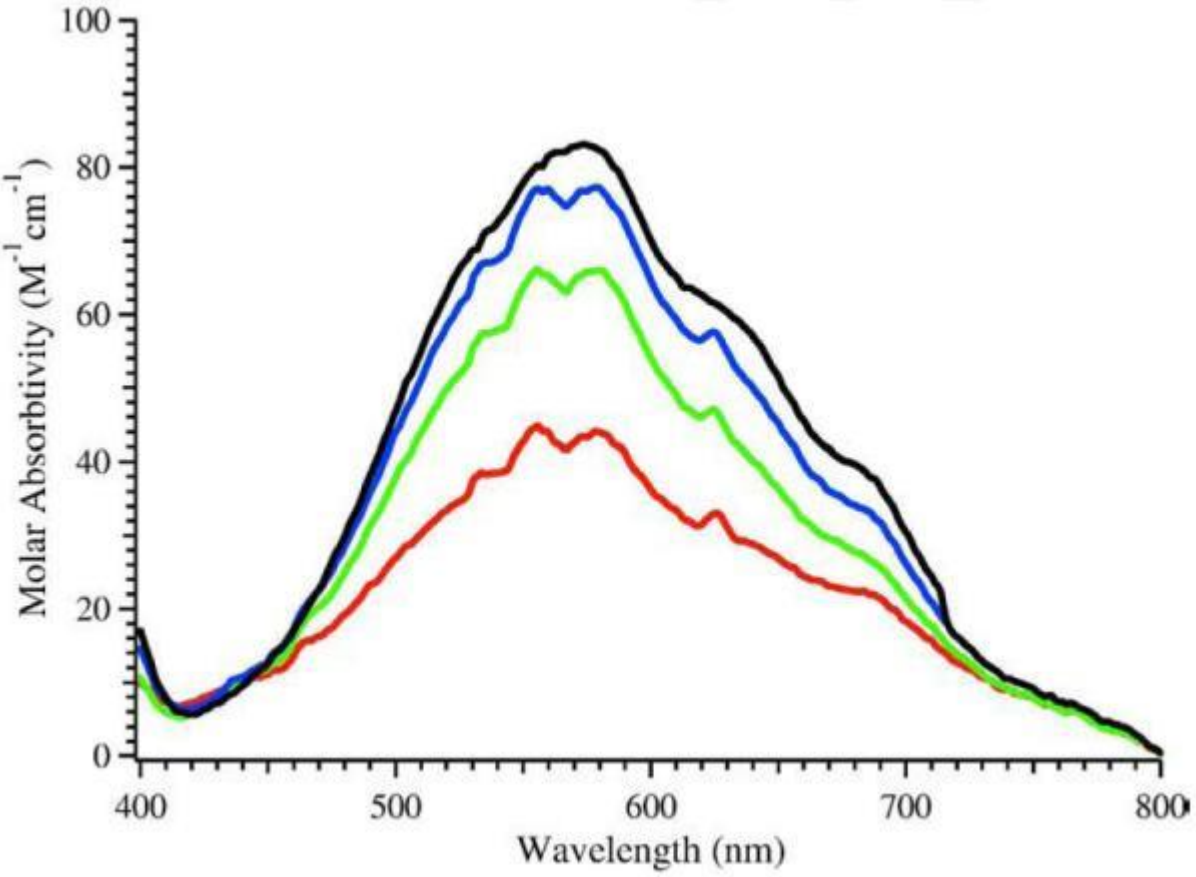

Fig. 5: Electronic absorption spectra of a 1 mM H63A *Ec*MetAP-I sample in 25 mM HEPES, pH 7.5, 150 mM KCl in the presence of 0.5 (red), 1.0 (green), 1.5 (blue), and 2 (black) equivalents of Co(II) at 25°C. (For interpretation of the references to colour in this figure legend, the reader is referred to the web version of this article.)

3. Discussion

MetAPs exhibit exclusive specificity for methionine residues located at the N-terminus of proteins and polypeptides [1-5]. All MetAPs appear to have similar substrate specificities, [5,30], in that MetAPs will *only* cleave N-terminal methionine residues that are adjacent to physically small and/or uncharged residues (*e.g.* G, A, P, S, T, C and V) [30]. In *Ec*MetAP-I, the S1 pocket is created by surface loops that include residues 59-68 and 221-224. The proposed substrate specificity pocket is lined by the hydrophobic residues C59, C70, Y62, Y65, Y168, F177, M206, W221, and Q233 [22,41]. Based on molecular modeling studies and sequence comparisons a flexible exterior loop near the active site of *Ec*MetAP-I was identified, which is made up of Y62, H63, G64, and Y65. This loop has been proposed to

Biochimica et Biophysica Acta: Proteins and Proteomics, Vol. 1794, No. 1 (January 2009): pg. 137-143. DOI.

play an important role in substrate binding and recognition and hence may regulate the type of N-terminal amino acid residue that is capable of binding to MetAPs. Inspection of the six X-ray crystal structures of MetAPs that have been reported thus far, reveal that a planar amino acid residue such as histidine (H63) or tyrosine forms a "cap" over the S1 pocket [17,20-25]. While this residue is not formally a member of the S1 binding pocket, it resides on a flexible surface loop and therefore may swing open or closed, thus regulating substrate binding. Based on X-ray crystal structures of *Ec*MetAP-I, residues in this flexible loop directly interact with active site bound inhibitors [22,41]. In order to investigate the role of H63 in substrate recognition and binding as well as its affect on the hydrolysis reaction catalyzed by *Ec*MetAP-I, we have generated the H63A *Ec*MetAP-I enzyme.

The specific activity of H63A *Ec*MetAP-I was determined using four different substrates of varying lengths, namely, l-Met-*p*-NA, MAS, MGMM and MSSHRWDW [33]. For the smallest/shortest substrate (l-Met-*p*-NA) the specific activity decreased nearly seven-fold. However, as the peptide length increased the specific activity also increased with H63A *Ec*MetAP-I exhibiting nearly full activity towards the octa-peptide MSSHRWDW. The observed decrease in specific activity is primarily due to a decrease in k_{cat} values, which drop nearly sixty-fold for l-Met-*p*-NA but only four-fold for the tri- and tetra-peptide substrates. Interestingly, no change in k_{cat} was observed when the octa-peptide MSSHRWDW was used as a substrate. Surprisingly, the H63A *Ec*MetAP-I enzyme could not hydrolyze l-Ala-*p*-NA or l-Leu-*p*-NA. These data indicate that as the peptide length increases, the effect of altering H63 on the catalytic process diminishes. Therefore, the observed kinetic changes are likely due to the lack of pre-organization of substrate and nucleophile for short peptides in the absence of H63. This conclusion is consistent with X-ray crystal structures of *Ec*MetAP-I which show that H63 forms direct contacts with inhibitor molecules bound in the active site [22,41]. Long peptides can overcome this lost interaction with H63 by added hydrophobic and hydrophilic bonding interactions, thereby decreasing the degree of positional and vibrational freedom.

Interestingly, k_{cat}/K_m values, which are a measure of substrate capture, follow an opposite trend to the observed k_{cat} values. For the smallest substrates, L-Met-*p*-NA and MAS, the observed k_{cat}/K_m values

Biochimica et Biophysica Acta: Proteins and Proteomics, Vol. 1794, No. 1 (January 2009): pg. 137-143. DOI.

decrease ~4.6-fold while MGMM decrease ~4.1-fold compared to WT *Ec*MetAP-I. However, for the longest peptide substrate, MSSHRWDW, the observed k_{cat}/K_m values are nearly identical to WT *Ec*MetAP-I. Even though the k_{cat} and K_m values for the four substrates tested are markedly affected by the elimination of H63, no major geometrical changes around the active site Co(II) ions are observed, based on electronic absorption and EPR spectra of Co(II)-loaded H63A *Ec*MetAP-I. These data indicate that H63 plays a role in substrate binding but that its role can be overcome when a longer peptide is used since the loss of one protein-substrate interaction can be overcome by many additional interactions. Additional insight into protein-substrate interactions can be gleaned from the X-ray crystal structure of a substrate-analog inhibitor ((3R)-amino-(2S)-hydroxy-heptanoyl- l-Ala- l-Leu- l-Val- l-Phe-OMe) bound to *Ec*MetAP-I (Figs. 1A, B). In this structure, the N-terminus of the inhibitor is coordinated to Co2, the keto oxygen (analogous to the carbonyl carbon in a terminal peptide bond) is ligated to Co1 and the (2S)-hydroxyl group displaces the bridging water/hydroxide ion [22,41]. The third residue, l-Leu, resides 3.7 Å away from H63 suggesting the formation of a hydrophobic interaction. Since the l-Leu side-chain resides in the S2 or S3 recognition pocket, the K_m values for long peptides are not greatly affected, as observed, since many additional hydrophilic and/or hydrophobic interactions exist. However, the loss of H63 would open up the S1 and S2 pockets to the solvent, which may allow new hydrophilic and/or hydrophobic interactions resulting in tighter substrate binding.

Recently, the X-ray crystal structure of *Sa*MetAP-I complexed with keto heterocycle or amino ketone inhibitors, revealed that the analogous residue to H63 in *Sa*MetAP-I becomes ordered and adopts a fixed conformation upon inhibitor binding [20]. The adopted conformation enlarged the S1 pocket and allowed the methyl group in the methionine side chain of each inhibitor to adopt different orientations corresponding to the possible rotamers [20]. Further inspection of the X-ray crystal structures of WT *Ec*MetAP-I in the absence and presence of (3R)-amino-(2S)-hydroxyheptanoyl- l-Ala- l-Leu- l-Val- l-Phe-OMe, suggest that H63 is quite labile and can adopt different conformations [22,41]. However, upon inhibitor binding the resulting hydrophobic interaction between H63 and l -Leucine forces the histidine residue to adopt a fixed conformation [22]. Therefore,

Biochimica et Biophysica Acta: Proteins and Proteomics, Vol. 1794, No. 1 (January 2009): pg. 137-143. DOI.

H63 likely plays a role in positioning the substrate as well as releasing the leaving group from the enzyme after hydrolysis has occurred. This proposal is also consistent with a previous report where H63 was mutated to leucine, resulting in no loss in the catalytic activity for *Ec*MetAP-I using MGMM as the substrate [42]. Combination of these data suggests that a large, planar side chain is important at position 63 in *Ec*MetAP-I and is also consistent with the observation that H63 (or a Y) is conserved in bacterial MetAP sequences (Fig. 2). Interestingly, in the mammalian type-I MetAP enzyme the corresponding loop containing the H63 residue is buried by an N-terminal extension, resulting in a decrease in flexibility for this loop [25]. Therefore, residues in this loop may provide a target for differentiating bacterial type-I enzymes from their mammalian counterparts.

The metal binding and structural properties of the H63A *Ec*MetAP-I enzyme were also investigated in order to ascertain whether alteration of H63 affects the dinuclear active site in *Ec*MetAP-I. The H63A *Ec*MetAP-I enzyme appears to bind one Co(II) ion tightly, similar to WT *Ec*MetAP-I, while a second metal ion is labile on the time scale of the buffer exchange (3 h, 4 °C) [28]. Dissociation constants (K_d) for Co(II) binding to H63A *Ec*MetAP-I were determined by both kinetic and ITC measurements. Based on an activity titration data. H63A *Ec*MetAP-I is active after the addition of only one Co(II) ion, which binds with a K_d value of 0.15 μM, similar to WT *Ec*MetAP-I [28]. On the other hand, the K_d values obtained *via* ITC for Co(II) binding to H63A *Ec*MetAP-I was 5.8 μM, which is within error of that observed for WT *Ec*MetAP-I. The larger K_d value observed using ITC is due to a decrease in dissociation which is typical when substrate can bind to the active site. The K_d value observed for the second metal binding event of H63A *Ec*MetAP-I is ~ 2-fold lower than that observed for WT *Ec*MetAP-I. Even though the $\Delta G°$ values are identical for both the WT and the H63A *Ec*MetAP-I, the $\Delta H°$ and $T\Delta S°$ values are much lower for H63A *Ec*MetAP-I then that observed for WT *Ec*MetAP-I. These data correlate with activity measurements for H63A and WT *Ec*MetAP-I and strongly suggest that the first metal binding site accommodates the catalytically relevant metal ion. This seemingly unexpected correlation, as H63 is not a direct ligand to the metal ions, underscores the importance of second-shell interactions in the active site of metalloenzymes.

Biochimica et Biophysica Acta: Proteins and Proteomics, Vol. 1794, No. 1 (January 2009): pg. 137-143. DOI.

It should be noted, however, that activity assays carried out on H63A *Ec*MetAP-I and WT *Ec*MetAP-I used enzyme concentrations of ~ 20 μM, which is two orders of magnitude larger than the K_d value determined for the first metal binding site of 0.2 or 0.4 μM assuming Hill coefficients of 1.3 and 2.1, respectively [43,44]. However, a K_d value of between 2.5 and 4.0 μM was reported when it was assumed that only a single Co(II) binding site exists in the low concentration regime, which is within error of ITC derived K_d values. Under the conditions utilized, any cooperativity in divalent metal binding will not be detectable in ITC experiments due to high enzyme concentrations (~70 μM) but may appear in EPR data. In fact, EPR data recorded on Mn(II)-loaded *Ec*MetAP-I and *Pf*MetAP-II suggests a small amount of dinuclear site formation even after the addition of only a quarter equivalent of Mn(II) [28,45,46]. Since activity titrations and ITC data are not particularly sensitive to the type of binding (i.e. cooperativity *vs.* two independent binding sites) the weak cooperativity observed by Larrabee et al.[43] and Hu et al. [44] would not be observed in these experiments but is entirely consistent with EPR data and, indeed, with the X-ray crystallographic data. Most X-ray structures of MetAPs were determined with a large excess of divalent metal ions so only dinuclear sites are observed. However, crystallographic data obtained on *Ec*MetAP-I using metal ion:enzyme ratios of 0.5:1 reveals Mn(II) ion occupancies of 71% bound to the M1 site and 28% bound to the M2 site, consistent with cooperative binding [27].

In conclusion, combination of kinetic, ITC, and spectroscopic data has allowed the mechanistic role of H63 in *Ec*MetAP-I to be examined. Alteration of H63 to an alanine residue primarily alters k_{cat} but also affects the K_m values of short peptide substrates. The observed change in k_{cat}, and consequently K_m, is likely due to the lack of pre-organization of substrate and nucleophile for short peptides in the absence of H63. Based on X-ray crystal structures of MetAP enzymes in the absence and presence of peptide inhibitors, H63 can form hydrophobic interactions with peptide bound to the dinuclear active site of MetAPs thereby adopting a more fixed conformation upon inhibitor binding. Since the dinuclear active site is not altered upon changing H63 to an alanine, the observed pertubrations in k_{cat} and K_m are not due to interactions with the active site metal ions. These data indicate that the residues situated on the flexible loop made up of Y62, H63, G64, and Y65 do, in fact, play an important role in substrate

Biochimica et Biophysica Acta: Proteins and Proteomics, Vol. 1794, No. 1 (January 2009): pg. 137-143. DOI.

binding and recognition in MetAP enzymes and may also provide a target with which to differentiate bacterial MetAPs from their mammalian counterparts.

Abbreviations

EcMetAP-I	methionine aminopeptidase from *Escherichia coli (E. coll)*
PfMetAP-II	methionine aminopeptidase from *Pyrococcus furiosus*
HEPES	[4-(2-hydroxyethyl)-1-piperazineethanesulfonic acid]
ICP-AES	Inductively coupled plasma-atomic emission spectroscopy
ITC	Isothermal titration calorimetry

Footnotes

⋆This work was supported by the National Science Foundation (CHE-0652981, RCH) and the National Institutes of Health (AIO56231, BB). The Bruker Elexsys spectrometer was purchased by the Medical College of Wisconsin and is supported with funds from the National Institutes of Health (NIH, EB001980, BB).

References

[1] Meinnel T, Mechulam Y, Blanquet S. Methionine as translation start signal — a review of the enzymes of the pathway in *Escherichia coli*. Biochimie. 1993;75:1061–1075.
[2] Arfin SM, Bradshaw RA. Cotranslational processing and protein turnover in eukaryotic cells. Biochemistry. 1988;27(21):7979–7984.
[3] Bradshaw RA. Protein translation and turnover in eukaryotic cells. TIBS. 1989;14:276–279.
[4] Bradshaw RA, Brickey WW, Walker KW. N-terminal processing: the methionine aminopeptidase and N^{α}-acetyl transferase families. TIBS. 1998;23:263–267.
[5] Lowther WT, Matthews BW. Structure and function of the methionine aminopeptidases. Biochim. Biophys. Acta. 2000;1477:157–167.
[6] Sherman F, Stewart JW, Tsunasawa S. Methionine or not methionine at the beginning of a protein. BioEssays. 1985;3:27–31.
[7] Chang S-YP, McGary EC, Chang S. Methionine aminopeptidase gene of *Escherichia coli* is essential for cell growth. J. Bacteriol. 1989;171(7):4071–4072.

[8] Chang Y-H, Teichert U, Smith JA. Molecular cloning, sequencing, deletion, and overexpression of a methionine aminopeptidase gene from *Sacchoromyces cerevistae*. J. Biol. Chem. 1992;267:8007–8011.

[9] Li X, Chang Y-H. Amino terminal protein processing in *Saccharomyces cerevisiae* is an essential function that requires two distinct methionine aminopeptidases. Proc. Natl. Acad. Sci. U. S. A. 1995;92:12357–12361.

[10] Miller CG, Kukral AM, Miller JL, Movva NR. *pepM* is an essential gene in *Salmonella typhimurium*. J. Bacteriol. 1989;171:5215–5217.

[11] Bradshaw R, Yi E. Methionine aminopeptidases and angiogenesis. Essays in Biol and Med. 2002;38:65–78.

[12] Sin N, Meng L, Wang MQW, Wen JJ, Bornmann WG, Crews CM. The anti-angiogenic agent fumagillin covalently binds and inhibits the methionine aminopeptidase, MetAP-2. Proc. Natl. Acad. Sci. U. S. A. 1997;94:6099–6103.

[13] Selvakumar P, Lakshmikuttyamma A, Lawman Z, Bonham K, Dimmock JR, Sharma RK. Expression of methionine aminopeptidase 2, N-myristoyltransferase, and N-myristoyltransferase inhibitor protein 71 in HT29. Biochem. Biophys. Res. Commun. 2004;322:1012–1017.

[14] Griffith EC, Su Z, Turk BE, Chen S, Chang Y-H, Wu Z, Biemann K, Liu JO. Methionine aminopeptidase (type 2) is the common target for angiogenesis inhibitors AGM-1470 and ovalicin. Chem. Biol. 1997;4:461–471.

[15] Griffith EC, Su Z, Niwayama S, Ramsay CA, Chang Y-H, Liu JO. Molecular recognition of angiogenesis inhibitors fumagillin and ovalicin by methionine aminopeptidase 2. Proc. Natl. Acad. Sci. U. S. A. 1998;95:15183–15188.

[16] Lowther WT, McMillen DA, Orville AM, Matthews BW. The anti-angiogenic agent fumagillin covalently modifies a conserved active site histidine in the *Escherichia coli* methionine aminopeptidase. Proc. Natl. Acad. Sci. U. S. A. 1998;95:12153–12157.

[17] Liu S, Widom J, Kemp CW, Crews CM, Clardy J. Structure of the human methionine aminopeptidase-2 complexed with fumagillin. Science. 1998;282:1324–1327.

[18] Taunton J. How to starve a tumor. Chem. Biol. 1997;4:493–496.

[19] Kruger EA, Figg WD. TNP-470: an angiogenesis inhibitor in clinical development for cancer. Exp. Opin. Invest. Drugs. 2000;9:1383–1395.

[20] Douangamath A, Dale GE, D'Arcy A, Almstetter M, Eckl R, Frutos-Hoener A, Henkel B, Illgen K, Nerdinger S, Schulz H, MacSweeney A, Thormann M, Treml A, Pierau S, Wadman S, Oefner C. Crystal structures of *Staphylococcus aureus* methionine aminopeptidase complexed with keto heterocycle and aminoketone inhibitors reveal

the formation of a tetrahedral intermediate. J. Med. Chem. 2004;47:1325–1328.

[21] Tahirov TH, Oki H, Tsukihara T, Ogasahara K, Yutani K, Ogata K, Izu Y, Tsunasawa S, Kato I. Crystal structure of the methionine aminopeptidase from the hyperthermophile, *Pyrococcus furiosus*. J. Mol. Biol. 1998;284:101–124.

[22] Lowther WT, Orville AM, Madden DT, Lim S, Rich DH, Matthews BW. *Escherichia coli* methionine aminopeptidase: implications of crystallographic analyses of the native, mutant and inhibited enzymes for the mechanism of catalysis. Biochemistry. 1999;38:7678–7688.

[23] Roderick LS, Matthews BW. Structure of the cobalt-dependent methionine aminopeptidase from *Escherichia coli*: a new type of proteolytic enzyme. Biochemistry. 1993;32:3907–3912.

[24] Spraggon G, Schwarzenbacher R, Kreusch A, McMullan D, Brinen LS, Canaves JM, Dai X, Deacon AM, Elsliger MA, Eshagi S, Floyd R, Godzik A, Grittini C, Grzechnik SK, Jaroszewski L, Karlak C, Klock HE, Koesema E, Kovarik JS, Kuhn P, McPhillips TM, Miller MD, Morse A, Moy K, Ouyang J, Page R, Quijano K, Rezezadeh F, Robb A, Sims E, Stevens RC, van den Bedem H, Velasquez J, Vincent J, von Delft F, Wang X, West B, Wolf G, Xu Q, Hodgson KO, Wooley J, Lesley SA, Wilson IA. Crystal structure of a methionine aminopeptidase (TM1478) from *Thermotoga maritima* at 1.9 A resolution. Proteins. 2004;56:396–400.

[25] Addlagatta A, Hu X, Liu JO, Matthews BW. Structural basis for the functional differences between type I and type II human methionine aminopeptidases. Biochemistry. 2005;44:14741–14749.

[26] Oefner C, Douangamath A, D'Arcy A, Hafeli S, Mareque D, Mac Sweeney A, Padilla J, Pierau S, Schulz H, Thormann M, Wadman S, Dale GE. The 1.15 A crystal structure of the *Staphylococcus aureus* methionyl-aminopeptidase and complexes with triazole based inhibitors. J. Mol. Biol. 2003;332:13–21.

[27] Ye QZ, Xie SX, Ma ZQ, Huang M, Hanzlik RP. Structural basis of catalysis by monometalated methionine aminopeptidase. Proc. Natl. Acad. Sci. U. S. A. 2006;103:9470–9475.

[28] D'souza VM, Bennett B, Copik AJ, Holz RC. Characterization of the divalent metal binding properties of the methionyl aminopeptidase from *Escherichia coli*. Biochemistry. 2000;39:3817–3826.

[29] Cosper NJ, D'souza V, Scott* R, Holz* RC. Structural evidence that the methionyl aminopeptidase from *Escherichia coli* is a mononuclear metalloprotease. Biochemistry. 2001;40:13302–13309.

[30] Ben-Bassat A, Bauer A, Chang S-Y, Myambo K, Boosman A, Chang S. Processing of the initiation methionine from proteins: properties of the

Biochimica et Biophysica Acta: Proteins and Proteomics, Vol. 1794, No. 1 (January 2009): pg. 137-143. DOI.

Escherichia coli methionine aminopeptidase and its gene structure. J. Bacteriol. 1987;169:751–757.

[31] Tobias JW, Shrader TE, Rocap G, Varshavsky A. The N-end rule in bacteria. Science. 1991;254:1374–1377.

[32] Ben-Bassat A, Bauer K. Amino-terminal processing of proteins. Nature. 1987;326:315.

[33] Meng L, Ruebush S, D'souza VM, Copik AJ, Tsunasawa S, Holz* RC. Overexpression and divalent metal binding studies for the methionyl aminopeptidase from *Pyrococcus furiosus*. Biochemistry. 2002;41:7199–7208.

[34] D'souza VM, Holz RC. The methionyl aminopeptidase from *Escherichia coli* is an iron(II) containing enzyme. Biochemistry. 1999;38:11079–11085.

[35] Mitra S, Dygas-Holz AM, Jiracek J, Zertova M, Zakova L, Holz RC. A new colorimetric assay for methionyl aminopeptidases: examination of the binding of a new class of pseudopeptide analog inhibitors. Anal. Biochem. 2006;357:43–49.

[36] Copik AJ, Swierczek SI, Lowther WT, D'souza V, Matthews BW, Holz RC. Kinetic and spectroscopic characterization of the H178A mutant of the methionyl aminopeptidase from *Escherichia coli*. Biochemistry. 2003;42:6283–6292.

[37] Bennett B, Holz RC. EPR studies on the mono- and dicobalt(II)-substituted forms of the aminopeptidase from *Aeromonas proteolytica.* Insight into the catalytic mechanism of dinuclear hydrolases. J. Am. Chem. Soc. 1997;119:1923–1933.

[38] Bennett B, Holz RC. Spectroscopically distinct cobalt(II) sites in heterodimetallic forms of the aminopeptidase from *Aeromonas proteolytica*: characterization of substrate binding. Biochemistry. 1997;36:9837–9846.

[39] Drago RS. Physical Methods for Chemists. 2nd ed Saunders; Orlano, FL: 1992.

[40] Segel IH. Enzyme Kinetics: Behavior and Analysis of Rapid Equilibrium and Steady-state Enzyme Systems. first ed. John Wiley & Sons; New York: 1975.

[41] Lowther TW, Zhang Y, Sampson PB, Honek JF, Matthews BW. Insights into the mechanism of *E. coli* methionine aminopeptidase from the structural analysis of reaction products and phosphorous-based transition state analogs. Biochemistry. 1999;38:14810–14819.

[42] Chiu C-H, Lee C-Z, Lin K-S, Tam MF, Lin L-Y. Amino acid residues involved in the functional integrity of the *Escherichia coli* methionine aminopeptidase. J. Bacteriol. 1999;181:4686–4689.

[43] Larrabee JA, Leung CH, Moore R, Thamrong-nawasawat T, Wessler BH. Magnetic circular dichroism and cobalt(II) binding equilibrium studies

of *Escherichia coli* methionyl aminopeptidase. J. Am. Chem. Soc. 2004;126:12316–12324.

[44] Hu XV, Chen X, Han KC, Mildvan AS, Liu JO. Kinetic and mutational studies of the number of interacting divalent cations required by bacterial and human methionine aminopeptidases. Biochemistry. 2007;46:12833–12843.

[45] Copik AJ, Nocek B, Swierczek SI, Ruebush S, SeBok J, D'souza VM, Peters J, Bennett B, Holz RC. EPR and X-ray crystallographic characterization of the product bound form of the Mn(II)-loaded methionyl aminopeptidase from *Pyrococcus furiosus*. Biochemistry. 2005;44:121–129.

[46] D'souza VM, Brown RS, Bennett B, Holz RC. Characterization of the active site and insight into the binding mode of the anti-angiogenesis agent fumagillin to the Mn(II)-loaded methionyl aminopeptidase from *Escherichia coli*. J. Biol. Inorg. Chem. 2005;10:41–50.

Supplementary Material

Mutation of H63 and Its Catalytic Affect on the Methionine Aminopeptidase from *Escherichia coli*†

Sanghamitra Mitra, Brian Bennett*, and Richard C. Holz*

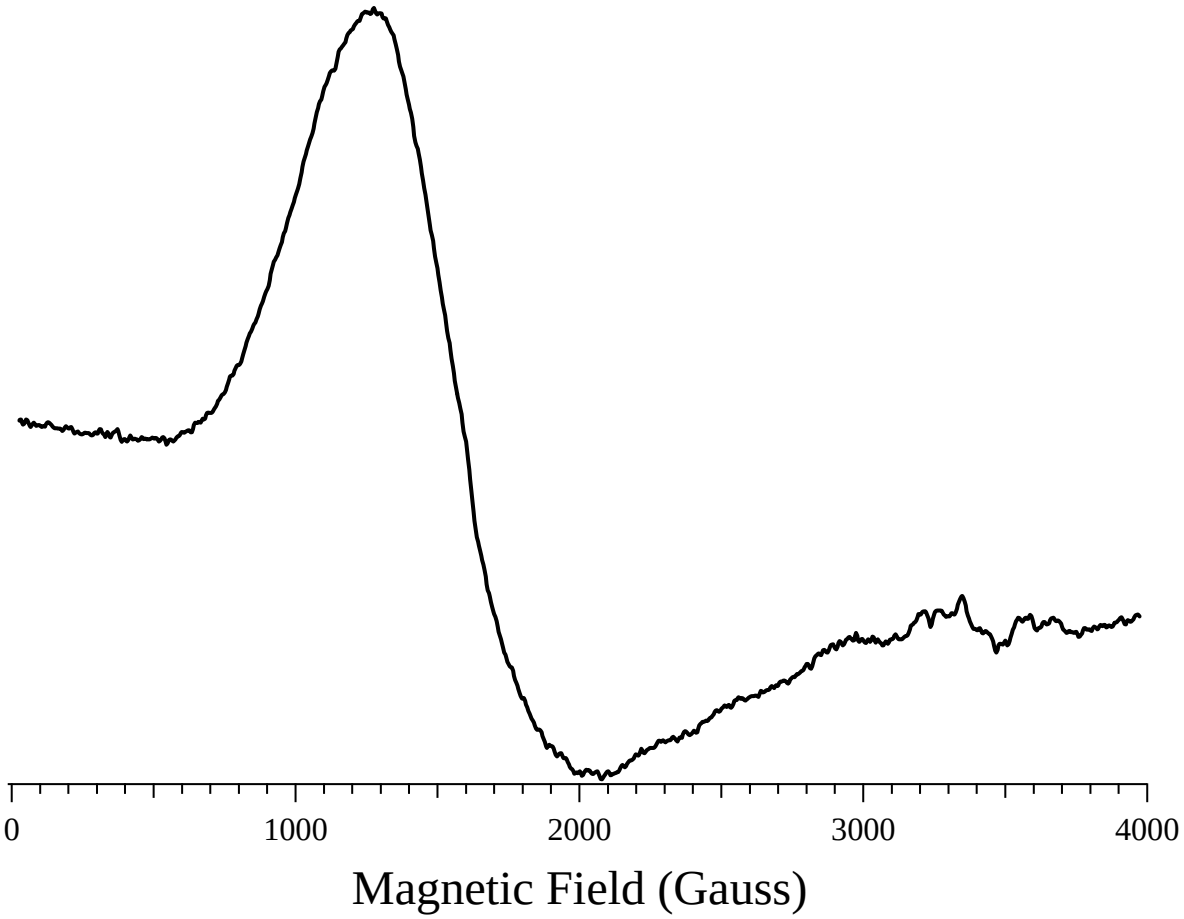

Figure S1. EPR spectrum of Co(II)-loaded H63A *Ec*MetAP-I. All the spectra were in 25 mM HEPES buffer and 150 mM KCl, pH 7.5, were recorded at 8 K, 0.2 mW microwave power, 1.2 mT field modulation amplitude, 100 kHz modulation frequency, and 10.2 mT s^{-1} sweep rate.

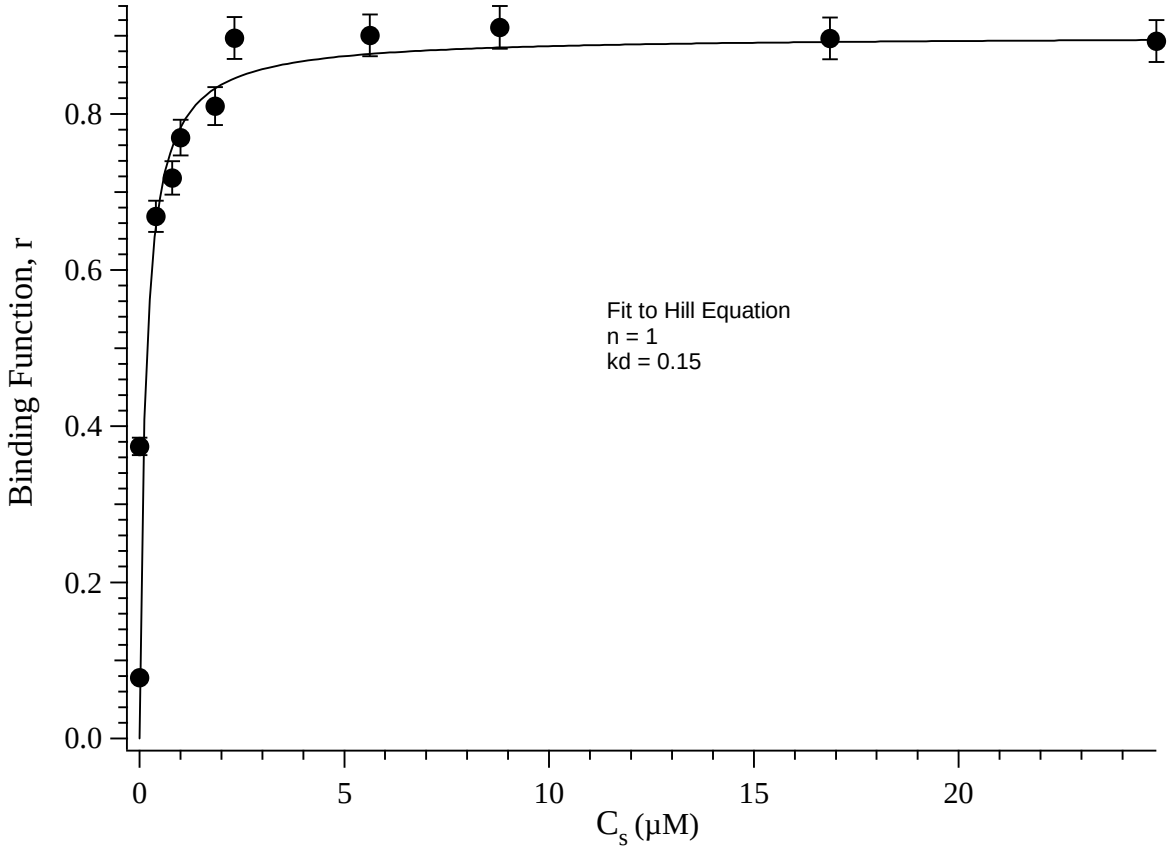

Figure S2. Plot of binding function, r vs. Cs for the binding of Co(II) to H63A *Ec*MetAP-I using MGMM as the substrate in HEPES buffer at pH 7.5. The solid line is a fit to the Hill Equation which provides an identical fit as that to eq. 3.